

## Supplementary Information for

### **Defective and ultrathin NiFe LDH nanosheets decorated on V-doped Ni<sub>3</sub>S<sub>2</sub> nanorod arrays: a 3D core-shell electrocatalyst for efficient water oxidation**

Jianqing Zhou,<sup>a‡</sup> Luo Yu,<sup>ab‡</sup> Qiancheng Zhu,<sup>a</sup> Chuqiang Huang,<sup>a</sup> and Ying Yu<sup>a\*</sup>

<sup>a</sup> College of Physical Science and Technology, Central China Normal University, Wuhan 430079, China

<sup>b</sup> Department of Physics and TcSUH, University of Houston, Houston, TX77204, USA

\* Corresponding author. Email: [yuying01@mail.ccnu.edu.cn](mailto:yuying01@mail.ccnu.edu.cn) (Y.Y)

‡ These authors contributed equally to this work.

## 1. Material synthesis

**Synthesis of V-Ni<sub>3</sub>S<sub>2</sub>.** The V-doped Ni<sub>3</sub>S<sub>2</sub> nanorod arrays was synthesized by a simple hydrothermal method. Firstly, a piece of Ni foam (2 x 4 cm) was ultrasonically cleaned by 2 M HCl solution, ethanol, and deionized water for 15 minutes each. Meanwhile, 60 mL reaction solution was prepared by dissolving 250 mg thioacetamide (TAA, CH<sub>3</sub>CSNH<sub>2</sub>) and 100 mg sodium orthovanadium (Na<sub>3</sub>VO<sub>4</sub>·12H<sub>2</sub>O) into deionized water. Secondly, Ni foam was immersed into the prepared solution and kept at 160 °C for 16 h in a sealed autoclave. Finally, the hydrothermal product was washed with deionized water and dried in air to obtain the V-doped Ni<sub>3</sub>S<sub>2</sub> nanorod arrays catalyst.

**Synthesis of V-Ni<sub>3</sub>S<sub>2</sub>@NiFe LDH.** The 3D core-shell V-Ni<sub>3</sub>S<sub>2</sub>@NiFe LDH electrocatalyst was fabricated by direct electrodeposition of NiFe LDH on as-prepared V-doped Ni<sub>3</sub>S<sub>2</sub> nanorod arrays according to previous method.<sup>1, 2</sup> Typically, the electrodeposition was conducted in a three-electrode system by using V-Ni<sub>3</sub>S<sub>2</sub> foam, Pt plate electrode and saturated calomel electrode as the working, counter, and reference electrode, respectively. A green mixture solution (0.15 M Ni(NO<sub>3</sub>)<sub>2</sub>·6H<sub>2</sub>O and 0.15 M FeSO<sub>4</sub>·7H<sub>2</sub>O) was used as electrolyte for the electrochemical preparation of NiFe LDH. The electrodeposition potential was -1.0 V vs SCE, and different deposition time with 40, 80, 120 s were used to control the thickness and morphology of the samples, which were marked as V-Ni<sub>3</sub>S<sub>2</sub>@NiFe LDH-40, V-Ni<sub>3</sub>S<sub>2</sub>@NiFe LDH-80, V-Ni<sub>3</sub>S<sub>2</sub>@NiFe LDH-120, respectively. In contrast, pure NiFe LDH was also grown on Ni foam by the same electrodeposition method with deposition time of 80 s. The mass loading of NiFe LDH was determined by weighing the sample before and after coating.

**Preparation of Pt/C electrode on Ni foam.** The commercial Pt/C (20 wt% Pt loading, Macklin, 15 mg) was mixed with 270 μL ethanol, 200 μL deionized water and 30 μL Nafion

solution, and the mixture was ultrasonicated for 30 min to obtain a homogeneous dispersion. Then the dispersed solution was coated onto nickel foam, followed with the dry in air at room temperature. The loading amount of Pt/C catalyst on the Ni foam is about 2.4 mg cm<sup>-2</sup>.

**Preparation of RuO<sub>2</sub> and IrO<sub>2</sub> electrode on Ni foam.** The benchmark RuO<sub>2</sub> electrode was prepared on Ni foam with the help of Nafion (5%) solution. Specifically, 10 mg RuO<sub>2</sub>, 50 μL Nafion, and 250 μL ethanol were mixed with ultrasonicated for 30 min to obtain a homogeneous dispersion. Then the dispersion solution was coated onto nickel foam, followed with the dry in air at room temperature. The loading of RuO<sub>2</sub> on Ni foam is about 2 mg cm<sup>-2</sup>. IrO<sub>2</sub> electrodes were prepared by the same method as the above.

## 2. Material characterizations

The morphology and phase composition of as-prepared catalysts were characterized by scanning electron microscope (SEM, JSM-6700F, 10 kV), transmission electron microscope (TEM) (Titan G2, 200 kV), X-ray diffraction (XRD, X'Pert PRO MRD, PANalytical, Netherlands). Raman spectra were collected by Raman spectrometer (LabRAM HR JY-Evolution) with 532 nm of green laser. The chemical state of catalyst was detected by XPS spectroscopy (VG Multiab-2000) using a PHI quantum 2000 system with charge neutralizer. Contact angle measurement was conducted on the JC2000-CG400 (POWEREACH). The gas product was determined by gas chromatography (GC-2014, Shimadzu, Japan).

## 3. Electrochemical measurements

The electrochemical tests were conducted on the electrochemical workstation (CHI660E) via a general three-electrode system in 1M KOH electrolyte. For detail, graphite rod and mercury oxide electrode (Hg/HgO) were used as counter electrode and reference electrode, respectively. All the obtained potentials vs Hg/HgO were converted to RHE according to Nernst

equation  $E_{\text{RHE}} = E_{\text{Hg/HgO}} + 0.0591 \text{ pH} + 0.098$ , and all the curves were reported with 95% IR compensation. In addition, all the polarization curves were obtained from the linear sweep voltammetry (LSV) test with a scan rate of 2 mV/s. Double-layer capacitance values were determined by cyclic voltammetry curve at different scan rate within a potential range of 0.385-0.485 V vs RHE. The plots of electrochemical impedance spectroscopy (EIS) were collected at an overpotential of 250 mV in the frequency of 0.1 Hz ~ 100 kHz.

#### 4. Supplementary figures

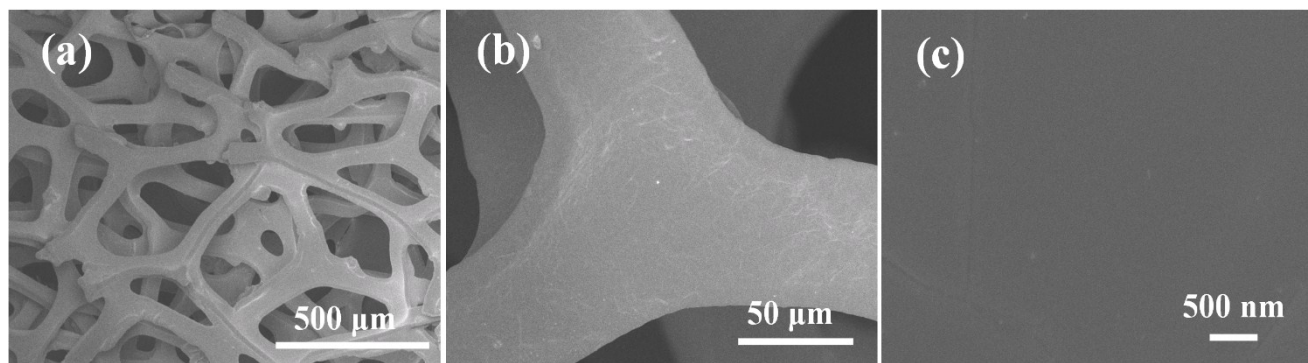


**Fig. S1** SEM images of commercial Ni foam at low and high magnifications.

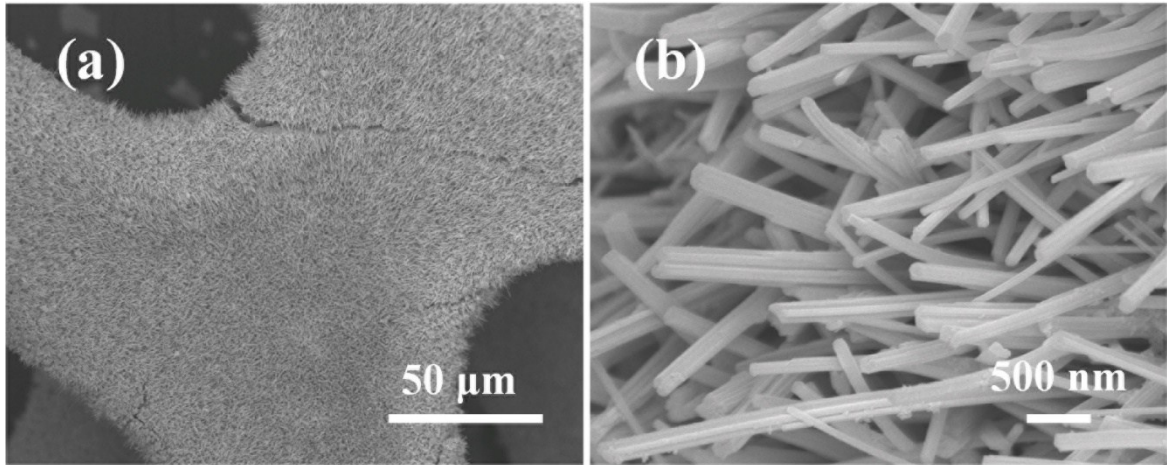


**Fig. S2** SEM images of V-Ni<sub>3</sub>S<sub>2</sub> nanorod arrays at low and high magnifications.

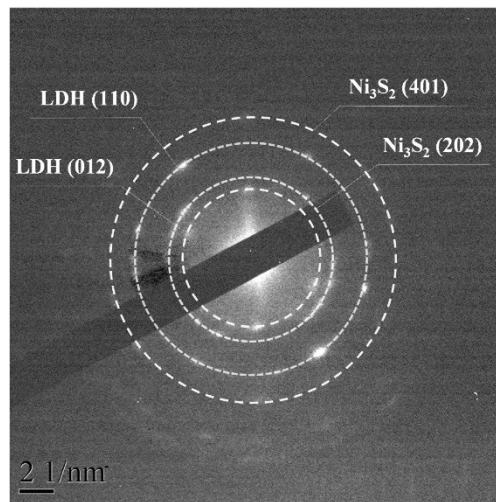


**Fig. S3** Selected area electron diffraction (SAED) of V-Ni<sub>3</sub>S<sub>2</sub>@NiFe LDH.

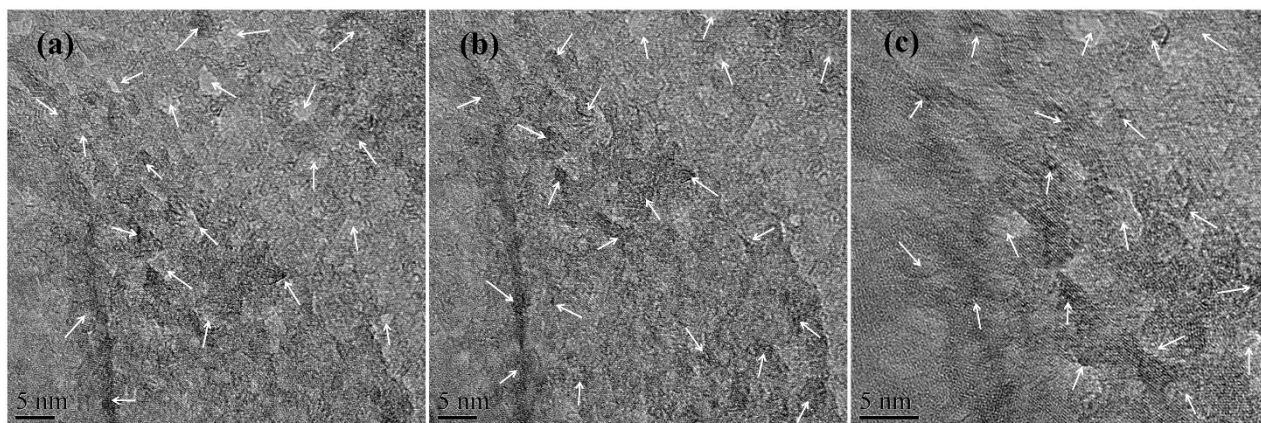


**Fig. S4** HRTEM image of defect-rich NiFe LDH on V-Ni<sub>3</sub>S<sub>2</sub>@NiFe LDH.

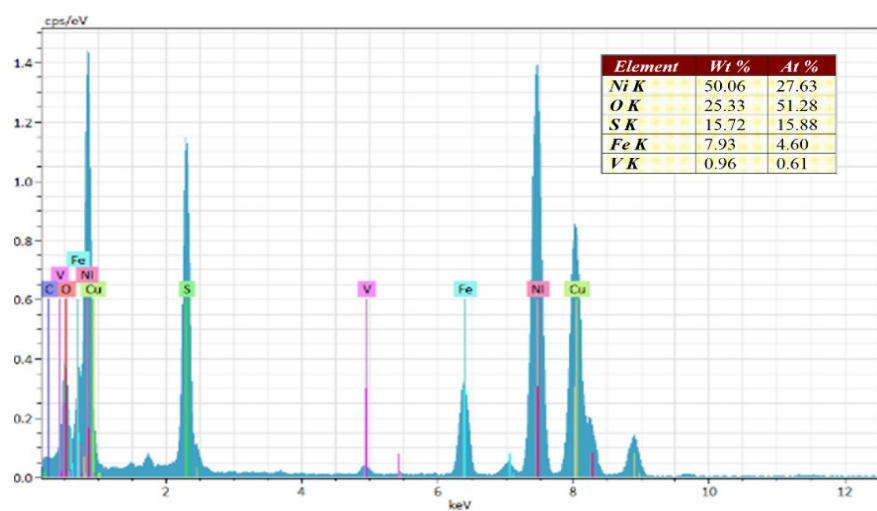


**Fig. S5** Energy dispersive X-ray (EDX) spectrum of V-Ni<sub>3</sub>S<sub>2</sub>@NiFe LDH.

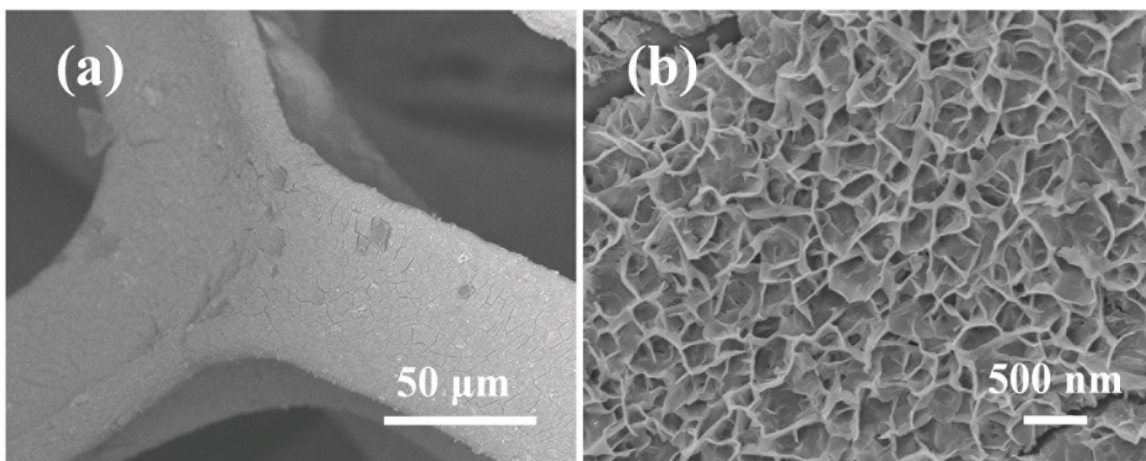


**Fig. S6** SEM images of pure NiFe LDH nanosheets at low and high magnifications.

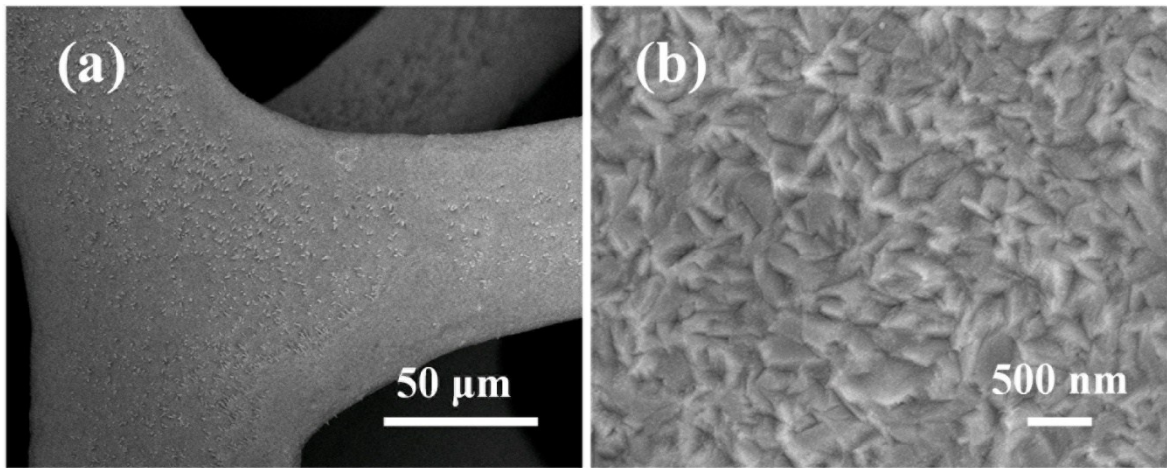


**Fig. S7** SEM images of pure Ni<sub>3</sub>S<sub>2</sub> at low and high magnifications.

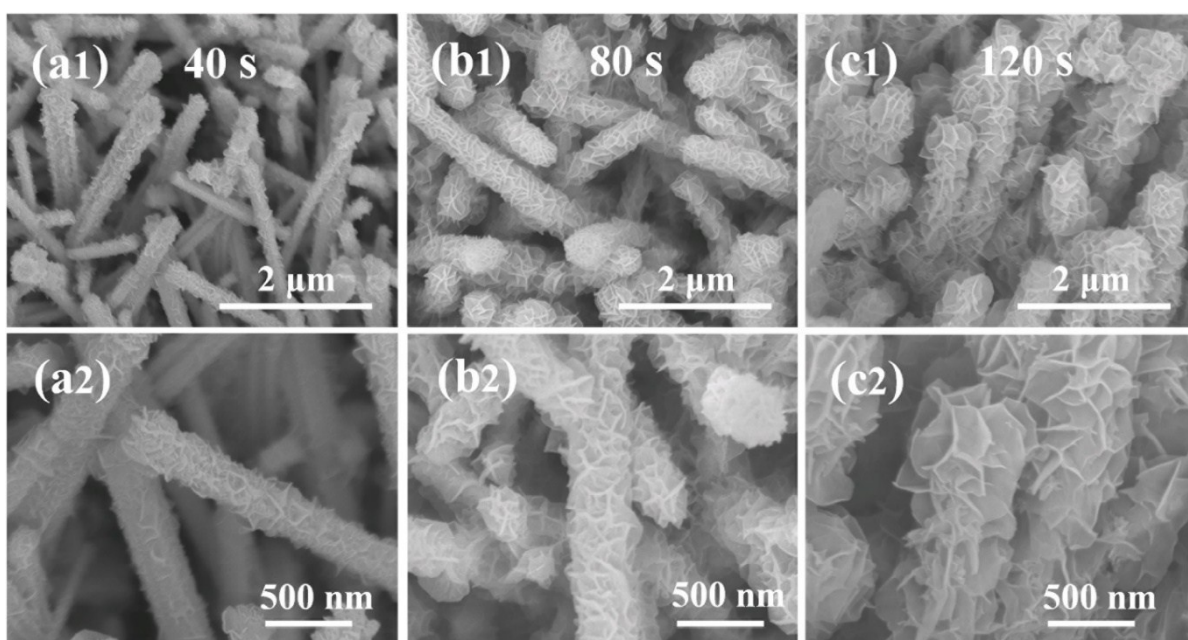


**Fig. S8** SEM images of (a1 and a2) V-Ni<sub>3</sub>S<sub>2</sub>@NiFe LDH-40, (b1 and b2) V-Ni<sub>3</sub>S<sub>2</sub>@NiFe LDH-80, and (c1 and c2) V-Ni<sub>3</sub>S<sub>2</sub>@NiFe LDH-120 at low and high magnifications.

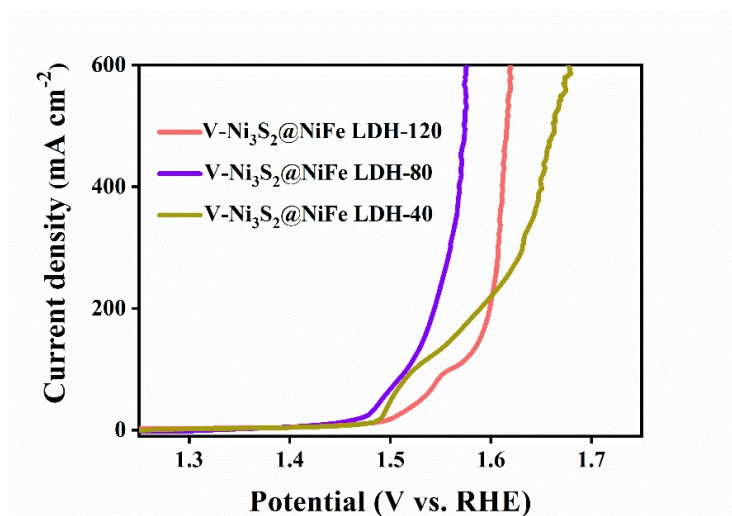


**Fig. S9** OER polarization curves of V-Ni<sub>3</sub>S<sub>2</sub>@NiFe LDH-40, V-Ni<sub>3</sub>S<sub>2</sub>@NiFe LDH-80, and V-Ni<sub>3</sub>S<sub>2</sub>@NiFe LDH-120.

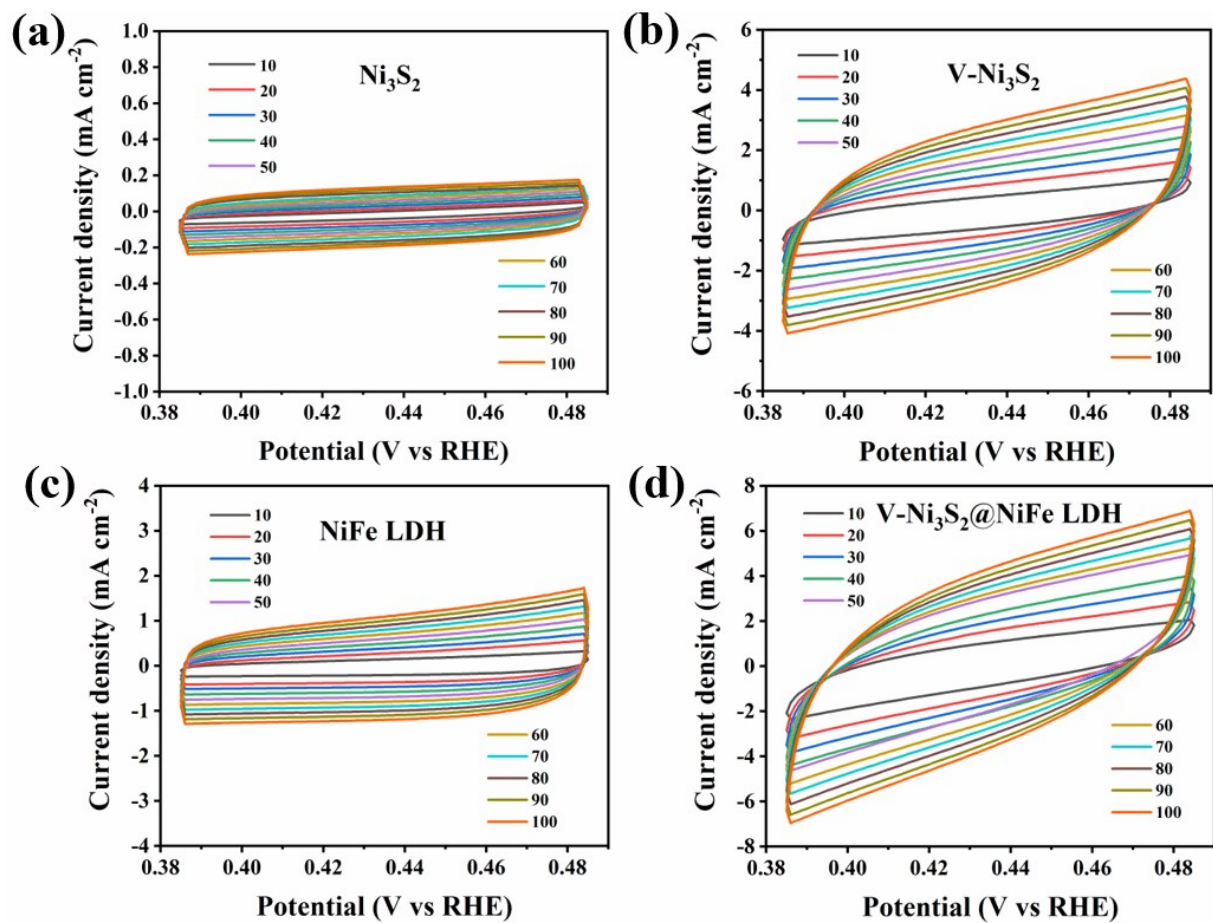


**Fig. S10** Cyclic voltammograms at different scan rates (from 10 mV/s to 100 mV/s with an interval rate of 10 mV/s). (a) Ni<sub>3</sub>S<sub>2</sub>, (b) V-Ni<sub>3</sub>S<sub>2</sub>, and (c) NiFe LDH, and (d) V-Ni<sub>3</sub>S<sub>2</sub>@NiFe LDH.

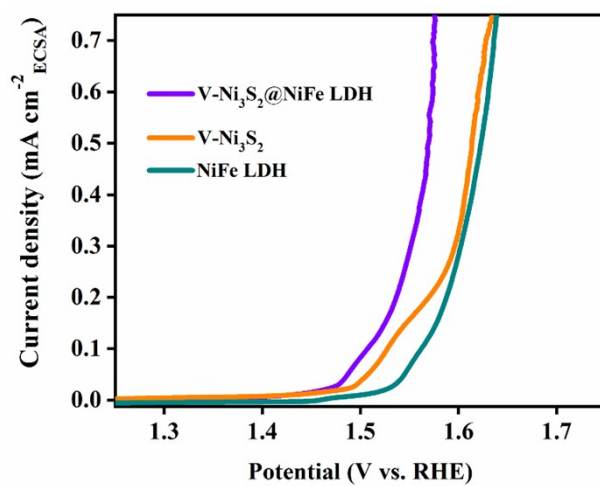


**Fig. S11** Polarization curves with current density normalized by the calculated ECSA for the different catalysts.

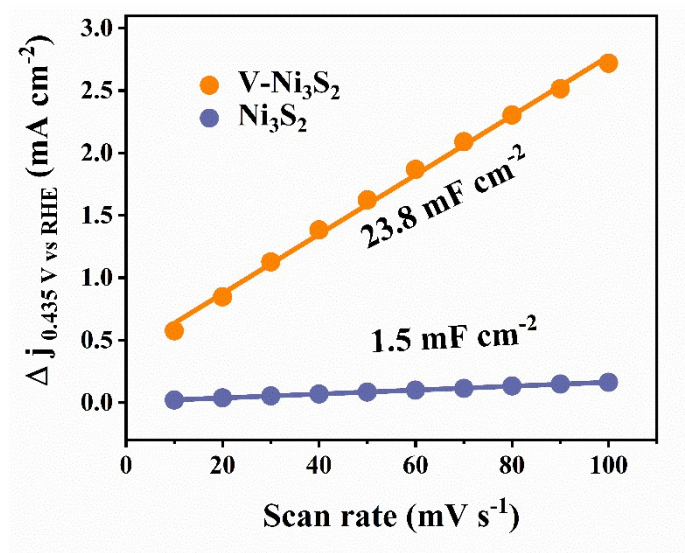


**Fig. S12** Capacitive current density as a function of scan rate for Ni<sub>3</sub>S<sub>2</sub> and V-Ni<sub>3</sub>S<sub>2</sub>.

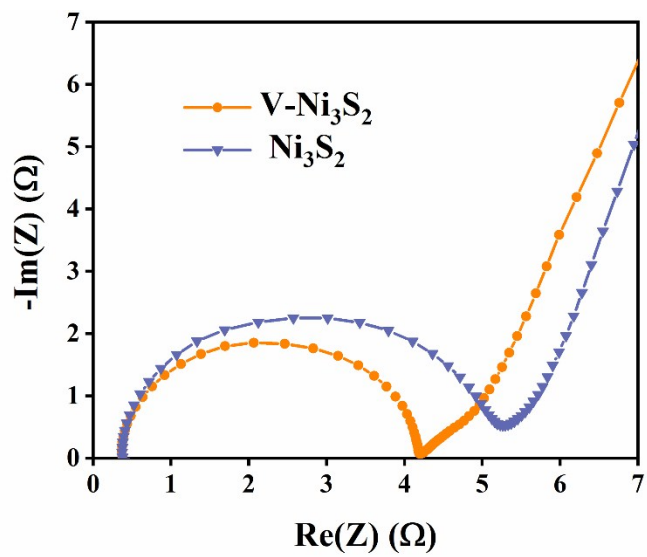
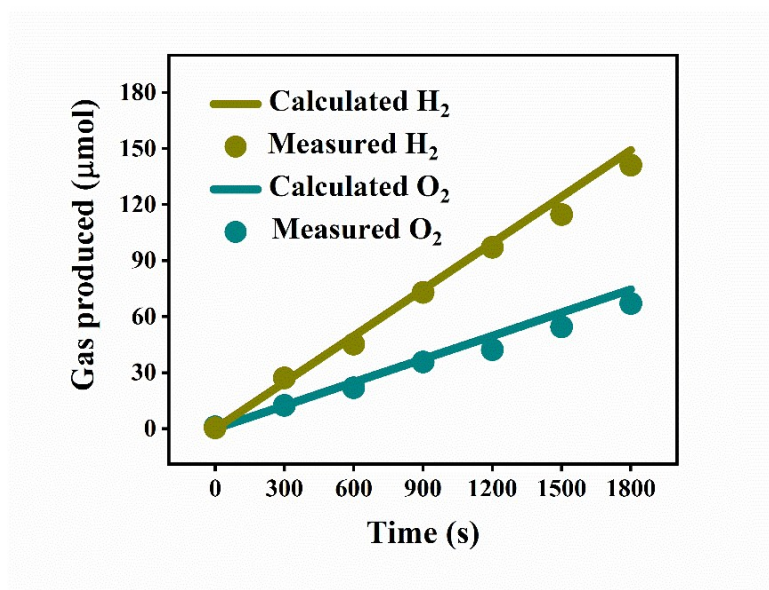
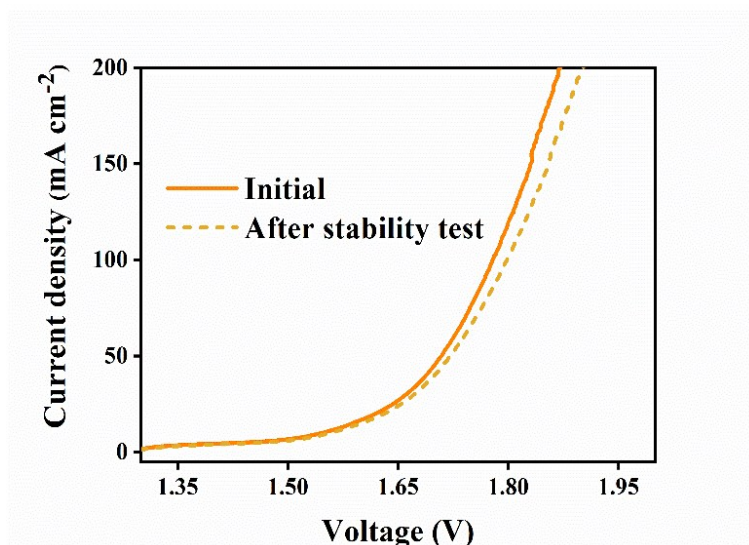


Fig. S13 Nyquist plots of  $\text{Ni}_3\text{S}_2$  and  $\text{V-Ni}_3\text{S}_2$ .



**Fig. S14** Experimental and theoretical calculated amounts of H<sub>2</sub> and O<sub>2</sub> by the overall water splitting of V-Ni<sub>3</sub>S<sub>2</sub>@NiFe LDH(+)//V-Ni<sub>3</sub>S<sub>2</sub>(-) at a current density of 50 mA cm<sup>-2</sup>.



**Fig. S15** Overall water splitting polarization curves before and after overall water splitting stability test.

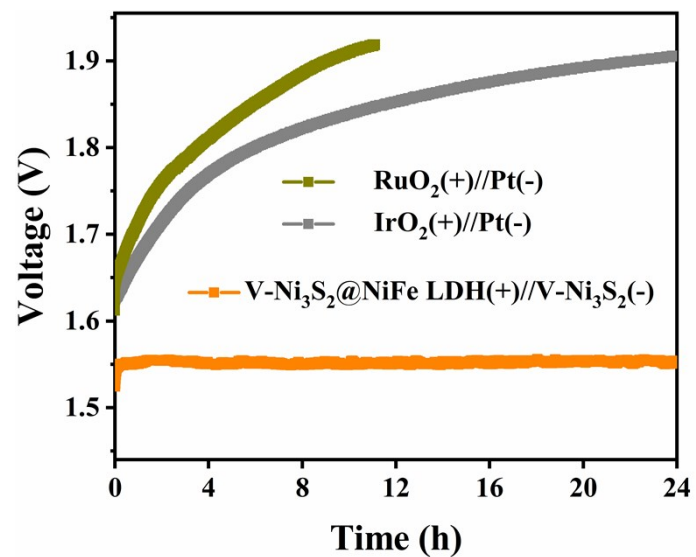


**Fig. S16** Stability tests of overall water splitting at a current density of 10 mA cm<sup>-2</sup> over different electrode pairs.

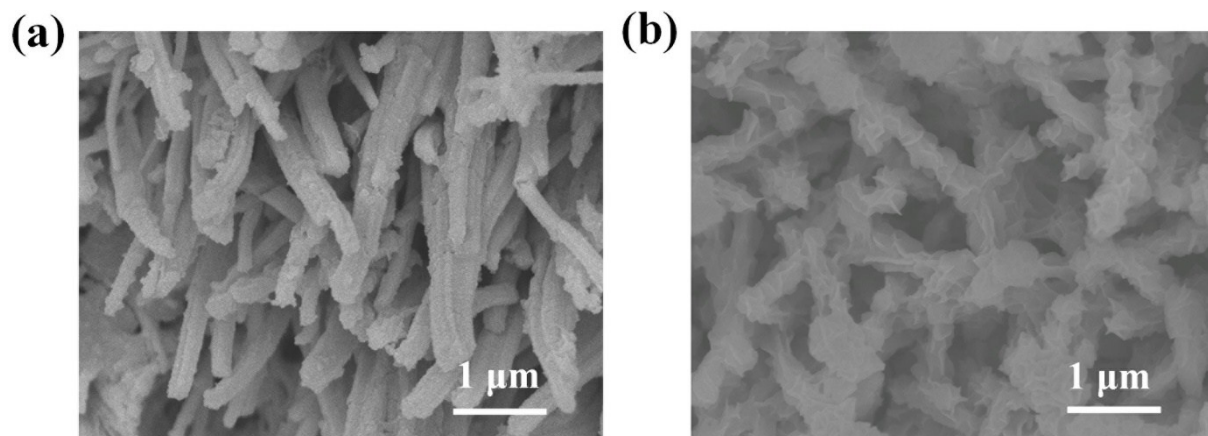


**Fig. S17** SEM images of (a) V-Ni<sub>3</sub>S<sub>2</sub> (cathode for HER) and (b) V-Ni<sub>3</sub>S<sub>2</sub>@NiFe LDH (anode for OER) after overall water splitting stability test.

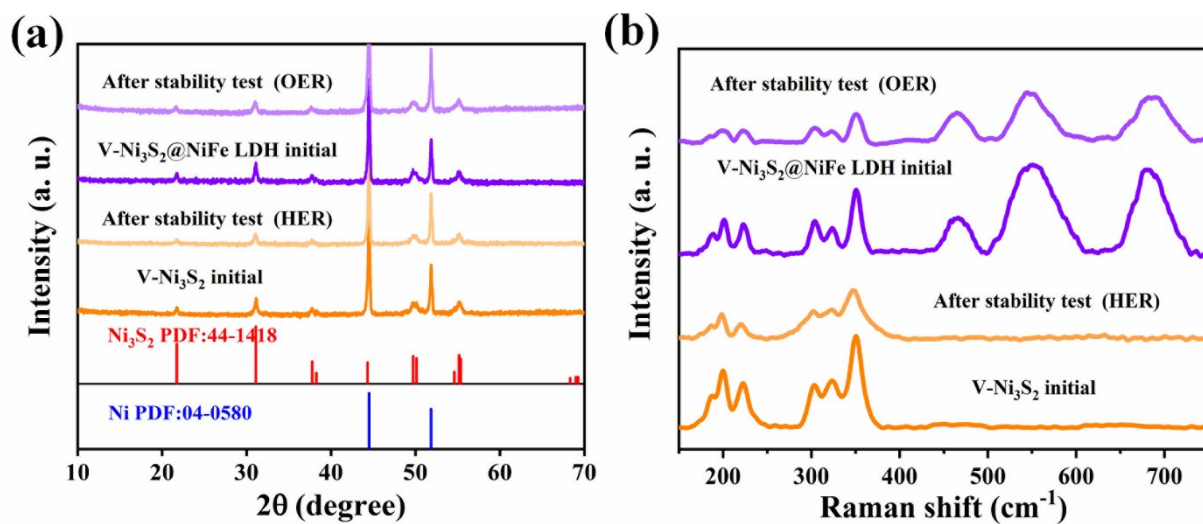


**Fig. S18** (a) XRD patterns, and (b) Raman spectra of V-Ni<sub>3</sub>S<sub>2</sub> and V-Ni<sub>3</sub>S<sub>2</sub>@NiFe LDH before and after overall water splitting stability test.

**Table S1.** Comparison of the OER performance for the V-Ni<sub>3</sub>S<sub>2</sub>@NiFe LDH catalyst with other reported OER electrocatalysts in 1 M alkaline electrolyte. The  $\eta_{10}$ ,  $\eta_{100}$ , and  $\eta_{300}$  correspond to the overpotentials at current densities of 10, 100, and 300 mA cm<sup>-2</sup>, respectively.

Catalysts	$\eta_{10}$ (mV)	$\eta_{100}$ (mV)	$\eta_{300}$ (mV)	Tafel slope (mV dec <sup>-1</sup> )	Reference
<b>V-Ni<sub>3</sub>S<sub>2</sub>@NiFe LDH</b>	<b>209</b>	<b>286</b>	<b>329</b>	<b>32.5</b>	<b>This work</b>
NiFe LDH	240	450*	NA	NA	<i>Science</i> <b>2014</b> , 345,1593-1596.
NiFe LDH/CNT	247	NA	NA	31	<i>J. Am. Chem. Soc.</i> <b>2013</b> , 135, 8452-8455.
NiFe LDH/graphene	210	325*	NA	52	<i>Adv. Mater.</i> <b>2017</b> , 29, 1700017.
Cu@CoFe LDH	240	300	NA	44.4	<i>Nano Energy</i> <b>2017</b> , 41, 327-336.
(Ni,Co) <sub>0.85</sub> Se/ NiCo LDH	216	285*	NA	85	<i>Adv. Mater.</i> <b>2016</b> , 28, 77-85.
CoSe/NiFe LDH	250	294*	NA	57	<i>Energy Environ. Sci.</i> <b>2016</b> , 9,478-483.
FeOOH/Co/FeOOH	NA	308	NA	32	<i>Angew. Chem. Int. Ed.</i> <b>2016</b> , 55,3694-3698.
Pt-NiFe LDH	230	310*	NA	333	<i>Nano Energy</i> <b>2017</b> , 39, 30-43.
Ni <sub>5</sub> P <sub>4</sub> /Ni <sub>5</sub> P <sub>2</sub> /NiFe LDH	197	243	283	46.6	<i>J. Mater. Chem. A.</i> <b>2018</b> , 6,13619-13623.
NiCo LDH/CFP	307	370*	410*	64	<i>Carbon</i> <b>2016</b> , 110, 1-7.
NiCo/NiCoO <sub>x</sub> @FeOOH	278	430*	NA	47.5	<i>Electrochim. Acta</i> <b>2017</b> ,257, 1-8.
NiFeRu LDH/Ni foam	225	265*	280*	32.4	<i>Adv. Mater.</i> <b>2018</b> , 30, 1706279.
NiFe LDH@Au/Ni foam	NA	235	250*	48.4	<i>ACS Appl. Mater. Interfaces</i> <b>2017</b> , 9, 19807-19814
NiFe LDH@NiCoP/NF	220	NA	550*	48.6	<i>Adv. Funct. Mater.</i> <b>2018</b> , 28, 1706847.
Mn-Co oxyphoshlide	330	NA	NA	52	<i>Angew. Chem. Int. Ed.</i> <b>2017</b> , 56,2386-2389.
Ni-Co-P	270	348	NA	76	<i>Energy Environ. Sci.</i> <b>2018</b> , 11,872-880.
Fe <sub>x</sub> Co <sub>1-x</sub> OOH	266	NA	NA	30	<i>Angew. Chem. Int. Ed.</i> <b>2018</b> , 57,2672-2676.
Ni(OH) <sub>2</sub> /Ni <sub>3</sub> S <sub>2</sub> /NF	NA	490	NA	61.8	<i>J. Mater. Chem. A.</i> <b>2018</b> , 6,6938-6946.
NiFe LDH@NiCo <sub>2</sub> O <sub>4</sub> /NF	NA	390	NA	53	<i>ACS Appl. Mater. Interfaces</i> <b>2017</b> ,9, 1488-1495.
Ni <sub>x</sub> Co <sub>3-x</sub> S <sub>4</sub> /Ni <sub>3</sub> S <sub>2</sub> /NF	160	330	NA	95	<i>Nano Energy</i> <b>2017</b> , 35, 161-170.
MoS <sub>2</sub> -Ni <sub>3</sub> S <sub>2</sub> HNRs/NF	249	340	396*	57	<i>ACS Catal.</i> <b>2017</b> , 7, 2357-2366.
Mo <sub>x</sub> W <sub>1-x</sub> S <sub>2</sub> @Ni <sub>3</sub> S <sub>2</sub> /NF	285	NA	NA	90	<i>ACS Appl. Mater. Interfaces</i> <b>2017</b> ,9, 26066-26076.
Co <sub>1</sub> Mn <sub>1</sub> CH/NF	NA	349	392*	NA	<i>J. Am. Chem. Soc.</i> <b>2017</b> , 139, 8320-8328.
Ni <sub>2</sub> P/Ni <sub>3</sub> S <sub>2</sub> /NF	210	290	387*	62	<i>Nano Energy</i> <b>2018</b> , 51, 26-36.

**Table S2.** Comparison of the overall water splitting performance for the device composed of V-Ni<sub>3</sub>S<sub>2</sub>@NiFe LDH(+)//V-Ni<sub>3</sub>S<sub>2</sub>(-) catalyst with that reported in literatures.

Catalysts	Current density	Applied voltage	Electrolyte	Reference
V-Ni <sub>3</sub> S <sub>2</sub> @NiFe LDH(+)// V-Ni <sub>3</sub> S <sub>2</sub> (-)	10 mA cm <sup>-2</sup>	1.55 V	1M KOH	<b>This work</b>
NiFe LDH/Ni(+)// NiFe LDH/Ni (-)	10 mA cm <sup>-2</sup>	1.70 V	1M NaOH	<i>Science</i> <b>2014</b> , 345,1593-1596.
Cu@CoFe LDH(+)// Cu@CoFe LDH(-)	10 mA cm <sup>-2</sup>	1.68 V	1M KOH	<i>Nano Energy</i> <b>2017</b> , 41, 327-336.
CoFe@NiFe/NF(+)// CoFe@NiFe/NF(-)	10 mA cm <sup>-2</sup>	1.59 V	1M KOH	<i>Appl. Catal. B</i> <b>2019</b> , 253,131-139.
Pt-NiFe LDH(+)// Pt-NiFe LDH(-)	20 mA cm <sup>-2</sup>	1.56 V	1M KOH	<i>Nano Energy</i> <b>2017</b> , 39, 30-43.
MoS <sub>2</sub> -Ni <sub>3</sub> S <sub>2</sub> HNRs/NF(+)// MoS <sub>2</sub> -Ni <sub>3</sub> S <sub>2</sub> HNRs/NF(-)	10 mA cm <sup>-2</sup>	1.50 V	1M KOH	<i>ACS Catal.</i> <b>2017</b> , 7, 2357-2366.
Ni <sub>5</sub> P <sub>4</sub> /Ni <sub>5</sub> P <sub>2</sub> /NiFe LDH(+)// Ni <sub>5</sub> P <sub>4</sub> /Ni <sub>5</sub> P <sub>2</sub> (-)	10 mA cm <sup>-2</sup>	1.52 V	1M KOH	<i>J. Mater. Chem. A.</i> <b>2018</b> , 6,13619-13623.
NiCo/NiCoO <sub>x</sub> @FeOOH(+)// NiCo/NiCoO <sub>x</sub> (-)	10 mA cm <sup>-2</sup>	1.65 V	1M KOH	<i>Electrochim. Acta</i> <b>2017</b> ,257, 1-8.
Pt/C(+)//Ir/C(-)	10 mA cm <sup>-2</sup>	1.60 V	1M KOH	<i>Adv. Mater.</i> <b>2018</b> , 30, 1706279.
NiFe LDH-NS@DG(+)// NiFe LDH-NS@DG(-)	20 mA cm <sup>-2</sup>	1.50 V	1M KOH	<i>Adv. Mater.</i> <b>2017</b> , 29, 1700017.
NiFe LDH@NiCoP/NF(+)// NiFe LDH@NiCoP/NF(-)	10 mA cm <sup>-2</sup>	1.57 V	1M KOH	<i>Adv. Funct. Mater.</i> <b>2018</b> , 28, 1706847.
NiFe LDH@NiCo <sub>2</sub> O <sub>4</sub> /NF(+)// NiFe LDH@NiCo <sub>2</sub> O <sub>4</sub> /NF(-)	10 mA cm <sup>-2</sup>	1.60 V	1M KOH	<i>ACS Appl. Mater. Interfaces</i> <b>2017</b> ,9, 1488-1495.
Ni <sub>x</sub> Co <sub>3-x</sub> S <sub>4</sub> /Ni <sub>3</sub> S <sub>2</sub> /NF(+)// Ni <sub>x</sub> Co <sub>3-x</sub> S <sub>4</sub> /Ni <sub>3</sub> S <sub>2</sub> /NF(-)	10 mA cm <sup>-2</sup>	1.53 V	1M KOH	<i>Nano Energy</i> <b>2017</b> , 35, 161-170.
Ni(OH) <sub>2</sub> /Ni <sub>3</sub> S <sub>2</sub> /NF(+)// Ni(OH) <sub>2</sub> /Ni <sub>3</sub> S <sub>2</sub> /NF(-)	10 mA cm <sup>-2</sup>	1.57 V	1M KOH	<i>J. Mater. Chem. A.</i> <b>2018</b> , 6,6938-6946.
Mo <sub>x</sub> W <sub>1-x</sub> S <sub>2</sub> @Ni <sub>3</sub> S <sub>2</sub> /NF(+)// Mo <sub>x</sub> W <sub>1-x</sub> S <sub>2</sub> @Ni <sub>3</sub> S <sub>2</sub> /NF(-)	10 mA cm <sup>-2</sup>	1.62 V	1M KOH	<i>ACS Appl. Mater. Interfaces</i> <b>2017</b> ,9, 26066-26076.
Co <sub>1</sub> Mn <sub>1</sub> CH/NF(+)// Co <sub>1</sub> Mn <sub>1</sub> CH/NF(-)	10 mA cm <sup>-2</sup>	1.68 V	1M KOH	<i>J. Am. Chem. Soc.</i> <b>2017</b> , 139, 8320-8328.
Ni-Co-P HNBs(+)// Ni-Co-P HNBs (-)	10 mA cm <sup>-2</sup>	1.62 V	1M KOH	<i>Energy Environ. Sci.</i> <b>2018</b> , 11,872-880.

### Supplementary references

- 1 L. Yu, H. Zhou, J. Sun, F. Qin, F. Yu, J. Bao, Y. Yu, S. Chen and Z. Ren, *Energy Environ. Sci.*, 2017, **10**, 1820-1827.
- 2 Y. Oh, W. Yang, J. Tan, H. Lee, J. Park, and J. Moon, *Adv. Funct. Mater.*, 2019, **29**, 1900194.